 doi:10.20944/preprints202101.0160.v1

CytroCell: Valued Cellulose from Citrus Processing Waste

Antonino Scurria [1], Lorenzo Albanese [2], Mario Pagliaro [1], Federica Zabini [2], Francesco Giordano [1], Francesco Meneguzzo [2,*], and Rosaria Ciriminna [1,*]

[1] Istituto per lo Studio dei Materiali Nanostrutturati, CNR, via U. La Malfa 153, 90146 Palermo, Italy; antonino.scurria@ismn.cnr.it (AS); mario.pagliaro@cnr.it (MP); francesco.giordano@cnr.it (FG)

[2] Istituto per la Bioeconomia, CNR, via Madonna del Piano 10, 50019 Sesto Fiorentino, FI, Italy; federica.zabini@cnr.it (FZ); lorenzo.albanese@cnr.it (LA)

[5] * Correspondences: rosaria.ciriminna@cnr.it (RC); francesco.meneguzzo@cnr.it (FM)

Abstract: Named herein "CytroCell", the cellulosic material obtained via hydrodynamic cavitation of citrus processing waste in water is cellulose of low crystallinity, high porosity, good water holding capacity and good dispersibility in water. These properties, here demonstrated for the first time for lemon and grapefruit CytroCell, open the route to mass scale production of a useful functional material from a cheap and abundant biowaste. The process, indeed, does not require any pre-treatment of the raw material, and does not use acid, alkali, chemical oxidants or enzymes.

Keywords: cellulose; lemon; grapefruit; citrus processing waste; hydrodynamic cavitation; bioeconomy

1. Introduction

Citrus processing waste (CPW), namely citrus bagasse comprised of compressed peel, seeds and segmental membrane residual of the citrus juice industry has long been identified as a potential source of multiple valued bioproducts, including cellulose [1,2]. Multiple chemical routes have been developed for the extraction of citrus cellulose from said by-product, generally starting from treatment with soda to remove lignin and hemicellulose, either with ethylenediaminetetraacetic acid as chelating agent [3], or followed by bleaching with 4% H_2O_2 under basic condition at 90°C [4]. Noting that the main use of CPW from orange and grapefruit juice production plants (over 10 million tonnes per year only in the USA) is as low value cattle feed obtained by energy intensive drying of CWP, scholars in 2013 identified the integrated physico-chemical pretreatments of the biowaste, including high speed grinding and treatment with caustic soda as the main challenges to the industrial development of the citrus biorefinery [5].

Beyond microcrystalline cellulose, waste orange peel has long been studied as a source of nanocellulose, namely a nanostructured material of exceptional mechanical (and thermal) properties ideally suited, if available at low cost and large amounts, for potentially numerous industrial applications [6], including carmaking using nanocellulose-based composites. Routes to nanocellulose derived from citrus processing waste include the use of enzymes [7], microwaves [8] and acids [9].

So far industrially manufactured on small scale from bleached wood pulp in the form of nanofibrillated cellulose (also known as microfibrillated cellulose or cellulose nanofiber) after chemical delamination (fibrillation) of the cellulose fibers via TEMPO-mediated oxidation [9] (TEMPO is the 2,2,6,6-tetramethylpiperidine-1-oxyl radical which used at buffered, alkaline pH with hypochlorite selectively oxidises the primary alcohols of the glucose units [10]), nanofibrillated cellulose is chiefly used in the paperboard and packaging industry to manufacture paperboard enhanced with microfibrillated cellulose, in milk cartons for the dairy industry [11].

As put it by Guan and co-workers [6], the biomass pretreatment to remove all non-cellulosic material (lignin and pectin) from lignocellulosic biomass requiring numerous chemical and mechanical steps followed by nanocellulose extraction via acid hydrolysis generating large amounts

Preprints (www.preprints.org) | NOT PEER-REVIEWED | Posted: 8 January 2021 doi:10.20944/preprints202101.0160.v1

of wastewater, high energy consumption for mechanical process, or long reaction time for enzymatic hydrolysis, so far has impeded the mass scale production of an exceptionally versatile biomaterial.

Perhaps the cleanest processes reported so far are the stepwise microwave hydrothermal treatment of dried depectinated orange peel from 120 °C to 180 °C producing nanocellulose fibrils [8]; and the autoclaving of lime processing waste at 110-130 °C to remove hemicellulose and pectin followed by high shear (at 20,000 rpm for 15 min) and high pressure (at 40 MPa for 5 passes) homogenizing [12]. Though demonstrated on lab-scale at low dried peel load (1 g of dried peel mixed with 70 g of distilled water), the nanocellulose obtained via the microwave hydrothermal treatment of dried depectinated orange peel had a high water retention capacity varying between 16 and 20 g_{H_2O} g^{-1} but as deeply colored in brown due to the Maillard reaction products formed from the degradation/caramelization of sugars and their further reaction with residual proteins at the high temperatures employed [8].

Hydrodynamic cavitation (HC) is increasingly applied in the extraction of natural products from multiple biomass sources [13]. In 2019, our teams applied the method to the extraction of the main bioproducts of orange processing waste directly on semi-industrial scale, *i.e.* processing 42 kg of wet waste orange peel (WOP) obtained from the citrus juice industry in 120 L water [14]. Focusing our initial attention on the water-soluble products resulting from the extraction, we isolated a unique form of pectin (named "IntegroPectin") having a low degree of esterification (17%) and containing plentiful amounts of co-extracted orange flavonoids hesperidin and naringin raising global interest in HC as an efficient and highly scalable hesperidin production method for the prevention or treatment of COVID-19 [15]. Shortly afterwards, we extended the method on the same semi-industrial scale to lemon and grapefruit processing waste, isolating a lemon pectin showing exceptional antioxidant [16] and good antibacterial [17] properties, and a grapefruit pectin showing even higher and broad-spectrum bactericidal action [18].

The only investigation carried out on the insoluble, cellulose-rich fraction obtained from HC of waste orange peel showed that the HC process was able to effectively increase the methane generation from the solid residues of the WOP material, with a clear increasing trend during the hydrocavitation process up to the full exploitation of the respective biochemical methane potential (BMP) reaching +8% of the theoretical BMP for the hydrocavitated solid sample obtained after 270 min of cavitation [14]. Now, we report the first structural investigation of the cellulose-rich fraction isolated from the HC-based extraction of lemon and grapefruit industrial processing waste. This new biomaterial (see below) is named herein "CytroCell".

2. Results and Discussion

2.1 Textural properties

The physisorption isotherms showing N_2 adsorption at 77 K and at sub-atmospheric pressures in Figure 1 show that both lemon and grapefruit CytroCell are mesoporous materials (*caveat*: the high electrostatic charge on the surface of both celluloses allowed to solely use an aggregate rather than a powdered specimento carry out the experiments). The shape of the isotherms intermediate between type IV (irreversible type IV isotherm characteristic of mesoporous solids, with pore size >2 nm) and type II (reversible type II isotherm characteristic of macroporous solids with pore size >50 nm). The hysteresis loop of the resulting Type IVa isotherm for mesoporous materials with pore size >4 nm, located in the multilayer range of the isotherm, is associated with said capillary condensation [19].

Comparison of the pore size and specific pore volume obtained via the classical pore size model developed by Barret, Joyner and Halenda (BJH) from the adsorption and desorption branches of the isotherms, shows similar values for both celluloses, with the exception of the pore size of lemon CytroCell measured on the adsorption branch, which is 2 nm larger than the pore size measured on the desorption branch (entries 1 and 2 in Table 1).

Coupled to the shape of the isotherms, these results indicate that the structure citrus of CytroCell includes large and open mesopores with a broad size distribution as observed in the case of certain tropical wood aerogels [20]. The pore size from the desorption branch, indeed,

Preprints (www.preprints.org) | NOT PEER-REVIEWED | Posted: 8 January 2021 doi:10.20944/preprints202101.0160.v1

corresponds to the aperture (entrance) size of the pore, whereas the pore size distribution (Figure 2) obtained from the adsorption branch of the isotherm corresponds to the size of the cavity [21].

Table 1. Specific pore volume and pore size for lemon and grapefruit CytroCell

Entry	Sample	Specific pore volume (cm^3/g)	Pore size (nm)
1	Lemon CytroCell	0.137[a]	29.49[a]
2	Lemon CytroCell	0.137[b]	27.34[b]
3	Grapefruit CytroCell	0.117[a]	23.63[a]
4	Grapefruit CytroCell	0.125[b]	23.96[b]

[a]From the BHJ adsorption branch; [b]from the BHJ desorption branch

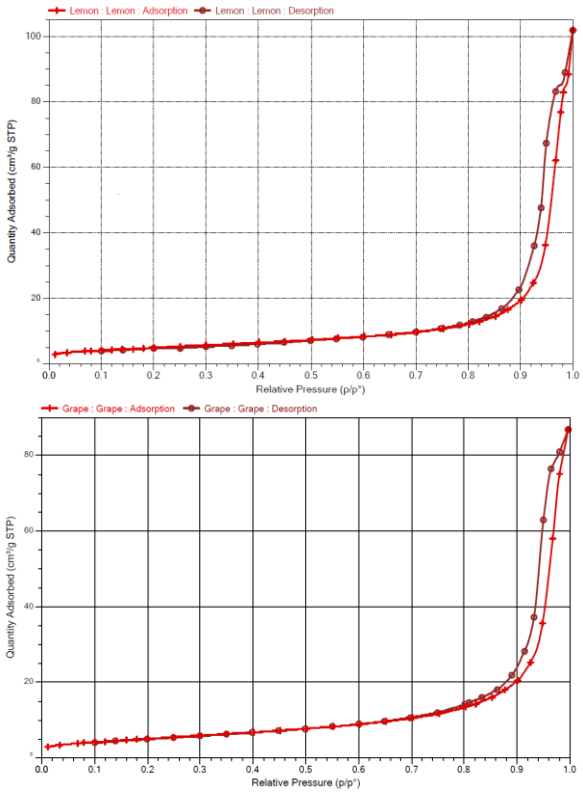

Figure 1. Low temperature N_2 adsorption-desorption isotherms for lemon (*top*) and grapefruit (*bottom*) CytroCell.

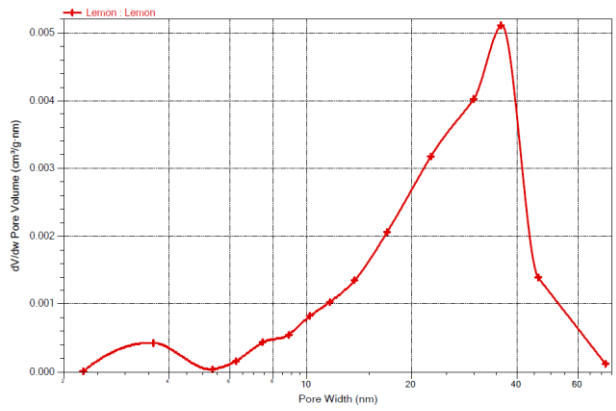

Preprints (www.preprints.org) | NOT PEER-REVIEWED | Posted: 8 January 2021 doi:10.20944/preprints202101.0160.v1

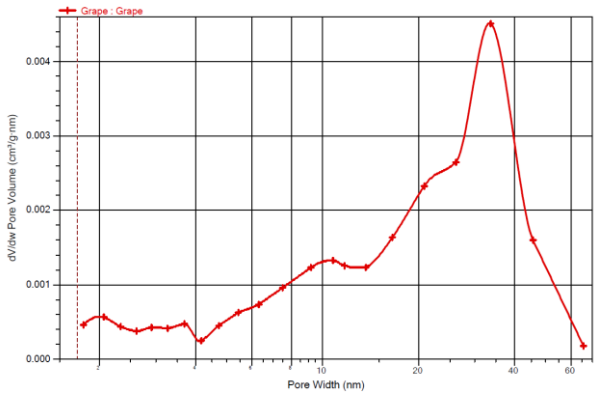

Figure 2. Pore size distribution for lemon (*top*) and grapefruit (*bottom*) CytroCell from the respective BJH isotherm desorption branch.

Likewise to the aforementioned tropical wood aerogels [20], the very narrow hysteresis loops in Figure 1, with the adsorption and desorption branches almost vertical and nearly parallel above 0.9 relative pressure, indicates the relatively large outer surface for both celluloses.

2.2 IR spectroscopy

The FTIR spectra in Figure 3 display all the characteristic cellulose peaks (Table 2), including those in the fingerprint region of 1000-1200 cm^{-1} [22,23].

Table 2. Selected absorption bands and corresponding vibrational modes of chemical groups in cellulose in the IR absorption spectrum of cellulose[a] [Adapted from Ref.22 and 23, CC BY license]

Wavenumber of absorption bands (cm^{-1})	**Chemical group**
3300-3400	νOH covalent bond, hydrogen bonding
2850-2925	νCH, νCH_2
1641	absorbed water (hydrogen-bonded)
1428	δCH_2 (symmetric) at C-6; crystalline region
1236	δCOH in plane at C-6
1160	νCOC at β-glycosidic linkage
1104	ν(C-O-C) in ring
1030	νCO at C-6
897	νCOC at β-glycosidic linkage, amorphous region
662	δCOH out of plane

[a]ν = stretching, δ = bending

The broad band around 3330-3400 cm^{-1} corresponds to the stretching vibrations of O–H bonds of free and bound water and O–H bonds of hydroxyl groups [24]. The bands at 2850-2925 cm^{-1} are due to the stretching vibrations of the C–H bonds in the saturated carbon rings of polysaccharides and to the stretching vibrations of these bonds in CH_2 groups [24]. The signal at 1160 cm^{-1} wavelenght derives from the stretching vibration of the C-O-C β-(1-4)-glycosidic bond as well as to the stretching vibrations of C–O bonds in saturated six-membered rings, whereas the signal at 897 cm^{-1} is due to νC-O-C at the same glycosidic linkage from the amorphous region of cellulose [25].

Preprints (www.preprints.org) | NOT PEER-REVIEWED | Posted: 8 January 2021 doi:10.20944/preprints202101.0160.v1

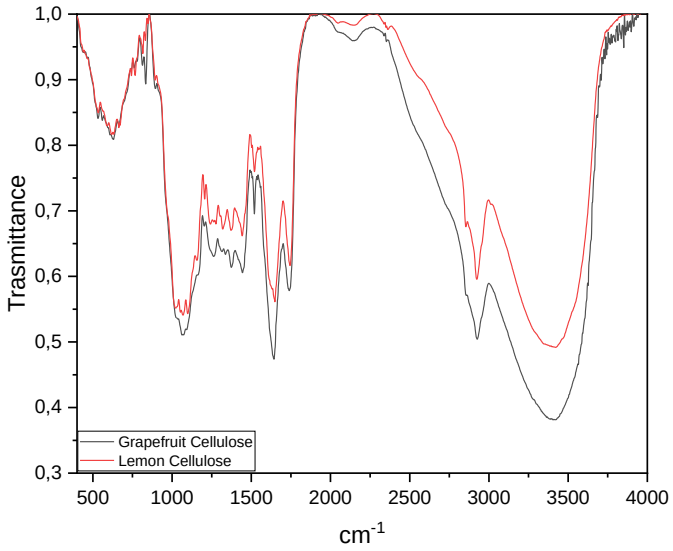

Figure 3. IR spectra for for lemon (*red*) and grapefruit (*black*) CytroCell.

The bands at 1650 cm^{-1} and at 1730 cm^{-1} are not due to pectin, which is efficiently separated from the lignocellulosic biomass and solubilized in water during the cavitation-based extraction process, but rather to the free and esterified carboxyl groups of cellulose esterified with citric acid upon reaction of the citric acid residual in the wet lemon (and in the wet grapefruit) bagasse and the primary alcohol groups of cellulose (Scheme 1) [26]:

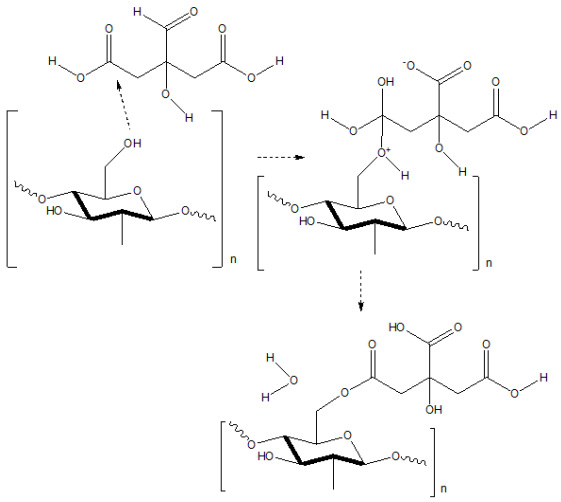

Scheme 1. Esterification of cellulose primary alcohol groups and citric acid.

Remarkably, the same peaks were observed and ascribed to the same esterified groups by scholars in Turkey analyzing a lemon resin obtained by boiling small pieces of lemon fruit [27], as well as by Brazilian scholars producing nanocellulose by reacting wood cellulose pulp with aqueous citric acid at 120 °C [28].

We make the hypothesis that the extreme conditions created in the imploding cavitation bubbles ease the reaction of citric acid with the primary hydroxyl group of cellulose chains to form an ester bond likewise to what happens in the latter process eventually affording partly esterified cellulose. Citric acid also play a crucial role also in converting the residual lignin in the waste citrus

Preprints (www.preprints.org) | NOT PEER-REVIEWED | Posted: 8 January 2021 doi:10.20944/preprints202101.0160.v1

peel by creating the "*in situ* catalytic environment" [8] similar to that of the microwave-assisted extraction able to hydrolyse lignin via proton transfer, β-elimination, and ester/ether cleavage [8].

2.3 X-Ray Diffraction

The XRD spectra in Figure 4 display all the characteristic diffraction peaks of cellulose from citrus waste with the 16.4° peak (101 plane), which can be separated into amorphous and crystalline portions, amorphous region between 16.4° and 18.0°, and the highest peak at 22.4° corresponding to diffraction from the 002 plane [29,8].

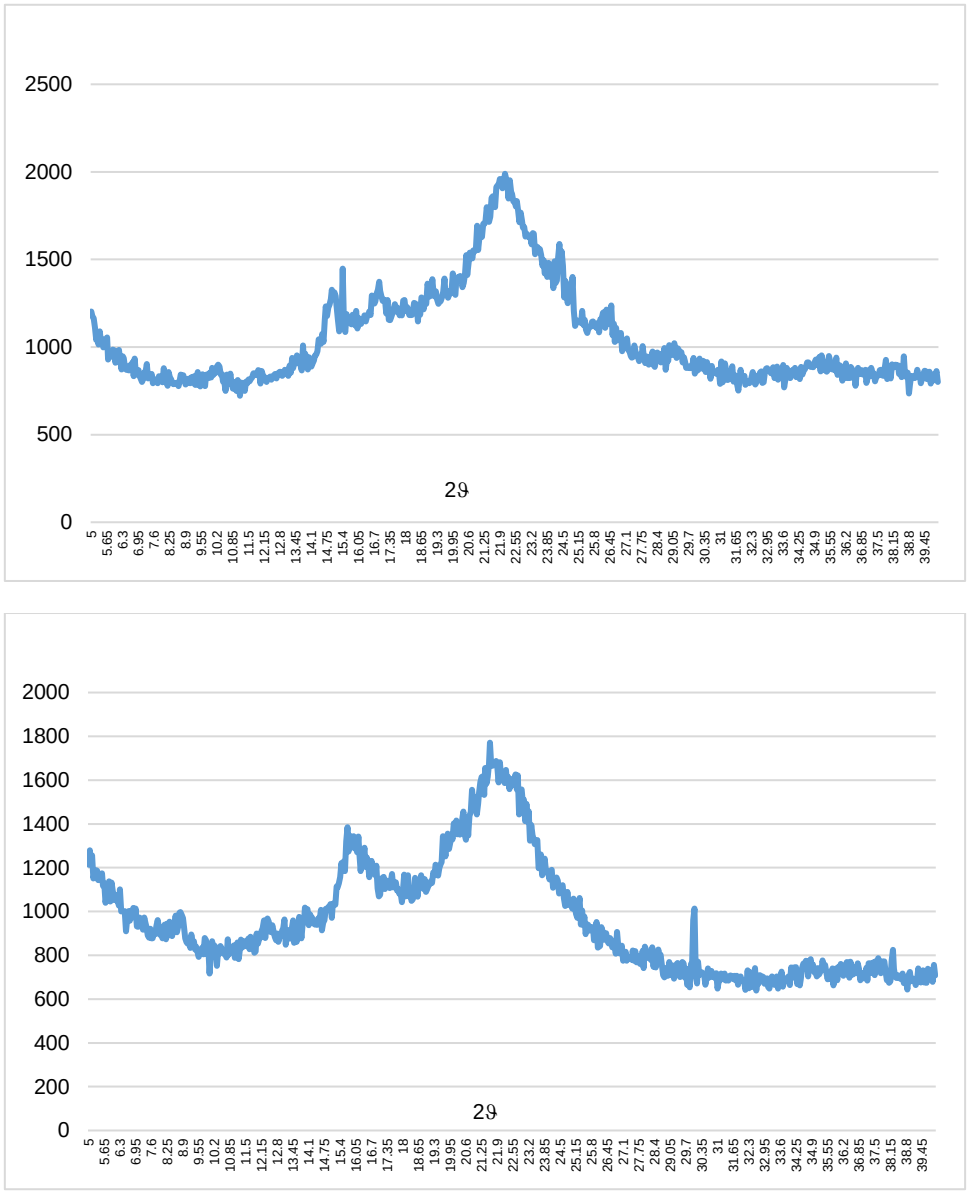

Figure 4. XRD spectra for for lemon (*top*) and grapefruit (*bottom*) CytroCell.

The crystallinity index (CI) readily calculated using the Segal equation (Eq.2), namely the ratio between the difference between the 002-peak intensity (I_{002}) and the intensity I_{am} of diffraction 2ϑ = 18° corresponding to the proportion of the amorphous cellulose [29]:

$$CI = (I_{002}-I_{am}))/I_{002} \quad (2)$$

Preprints (www.preprints.org) | NOT PEER-REVIEWED | Posted: 8 January 2021 doi:10.20944/preprints202101.0160.v1

Using the intensity arbitrary units from the diffractograms displayed in Figure 4, the aforementioned equation returns exceptionally low levels values for the CI of 0.33 for lemon CytroCell and 0.36 for grapefruit CytroCell:

CI (lemon CytroCell) = (1650-1100))/1650 = 0.33 (3)

CI (grapefruit CytroCell)= (1950-1250)/1950 = 0.36 (4)

This points to a key role of citric acid (far more abundant in lemon) during the hydrodynamic cavitation of the wet industrial waste of the citrus juice industry, in analogy to what observed in the conversion of the key citrus terpenes limonene and linalool [30]. For comparison, the crystallinity index of orange bagasse nanocellulose obtained upon enzymatic hydrolysis of bacterial cellulose is 0.63 [7], still significantly lower than that of cotton nanofibers having a CI of 0.78 [31]. Likewise to what observed for citrus depectinated nanocellulose obtained via microwave-assisted extraction [6], peaks at about 15°, 24° and 30° deriving from CaC_2O_4 are observed in the XRD spectra, particularly in the case of grapefruit CytroCell (Figure 4, bottom). Calcium oxalate crystals are ubiquitous in many plants (in widely different parts of the plant, from leaves to roots) where they exert multiple functions against both abiotic (drought, nutrient deprivation, metal toxicity) and biotic (pathogens and herbivore) stress factors [32].

2.4 Zeta potential

The results of the zeta potential, an indirect measure of the net charge of particles in suspension which indicates the stability of a suspension (the larger the ζ potential absolute value, the more stable the colloidal dispersion), displayed in Table 3 point to a negative value approaching -30 mV for lemon CytroCell and -23 mV for grapefruit CytroCell.

Table 3. ζ potential for lemon and grapefruit CytroCell obtained using hydrodynamic cavitation

Material	**Zeta Potential** (mV)
Lemon CytroCell	-29.5
Grapefruit CytroCell	-22.67

In agreement to guidelines classifying nanoparticle dispersions derived from the Derjaguin, Landau, Verwey, and Overbeek theory of colloids, this indicates that lemon CytroCell nanoparticles are highly stable ($\zeta > \pm 30$ mV), whereas grapefruit CytroCell particles ($\pm 20 < \zeta < 30$ mV) are moderately stable [33]. These values of the potential are close to those of wood nanocellulose obtained after the hydrothermal treatment of commercial cellulose with citric acid for 1.5 h (-36.5 mV [28]), ascribed to the presence of anionic carboxyl groups at the surface of nanocellulose, imparting increased electrostatic repulsion, and thus enhanced stability of the colloidal suspension.

2.5 Water Holding Capacity

We measured the water holding (or retention) capacity (WHC) for both grapefruit and lemon CytroCell by leaving for 30 min a sample of mildly dried CytroCell with distilled water in a centrifuge tube. After centrifugation, the water retention capacity of lemon CytroCell was 8 g_{water}/g_{cell} whereas that of grapefruit CytroCell was 5 g_{water}/g_{cell}. The water holding (or retention) capacity (of cellulose is a key parameter affecting the applications of cellulose in the food, pharmaceutical and cosmetic industries. In general, the WHC increases with increasing fiber length. For example for powedered cellulose (70% crystalline and 30% amorphous) the WHC quickly increases between 4 g_{water}/g_{cell} and 9.5 g_{water}/g_{cell} for fibers between 35 μm and 110 μm, whereas it remains virtually constant for fibers shorther than 35 μm and longer than 110 μm [34].

Preprints (www.preprints.org) | NOT PEER-REVIEWED | Posted: 8 January 2021 doi:10.20944/preprints202101.0160.v1

Figure 5. Disc of lemon CytroCell obtained upon mild drying of an aqueous paste.

Showing the large applicative potential of these new nanocelluloses due to their WHC, Figure 5 shows a disc of lemon CytroCell readily obtained upon mildly drying overnight at 35°C a dispersion of the material in water. The porous and fibrous nature of the a lightweight biomaterial is readily recognized.

3. Conclusions

We have discovered a new form of citrus cellulose of low crystallinity index, large open mesoporosity, good water retention capacity and dispersibility in water which can be easily synthesized in large amount by hydrodynamic cavitation of citrus processing biowaste. Named "CytroCell", this new form of nanocellulose herein studied starting from lemon and grapefruit bagasse has ultralow crystallinity of about 0.35, large mesoporosity (pore size close to or even exceeding 25 nm), and good water holding capacity approaching almost 10 g_{water}/g_{cell} in the case of lemon CytroCell). Part of the cellulose fibrils, we argue in this study, are esterified with citric acid, abundant in the wet residue of lemon and grapefruit industrial juice production used as raw material. The biomaterial obtained from the food industry waste rather than from wood pulp is suitable for a wide variety of applications. The large pore diameter around 24 nm for both celluloses, for example, makes them suitable for catalysis (as metal support), separation (chromatography) and adsorption (decontamination) using an intrinsically sustainable biomaterial.

Carried out in water only, the physical production route does not require any chemical reactant nor any pre-treatment of the raw material, thereby establishing an intrinsically green production route for cellulose starting from biobased waste available worldwide in over ~110–120 million tons annually worldwide [35] using an easily scalable and low operational expense process increasingly employed for the extraction of numerous natural products [13,14].

4. Experimental

4.1 Materials Preparation

The raw materials (integral aqueous extracts of lemon and grapefruit bagasse) were obtained from by means of hydrodynamic cavitation processes lasting 60 min as in previous experiments [14]. The cellulosic material was filtered using a Büchner filter with Whatman ashless filter paper, grade 589/3. The aqueous phase was used to isolate IntegroPectin via lyophilization [16] while CytroCell cellulose was isolated from the filtered wet solid phase. A filtrate sample (50 g) including plentiful adsorbed water was mixed with 150 mL of distillate water under fast stirring (470 rpm) for 30 min using a KS 260 control flat shaker (IKA-Werke, Staufen, Germany). The washed material was further refined pressing the cellulosic paste through the mesh of a laboratory test sieve (aperture of 212 μm,

 doi:10.20944/preprints202101.0160.v1

Endecotts, London, Great Britain) using a flat glass specimen. The refined material was dried in an oven at 35 °C for 20 h. The amount of isolated dried lemon and grapefruit CytroCell was 1.2 g and 1.7 g, respectively.

4.2 Water Holding Capacity

To measure the water retention capacity a sample of dried CytroCell (1 g) was mixed with 15 mL of deionized water and poured into two 20 mL centrifuged tubes. The two samples were stirred for 10 min and then centrifuged at 3000 rpm for 30 min using an Allegra X-22R benchtop centrifuge (Beckman Coulter, Palo Alto, CA, USA). After centrifugation, the supernatant aqueous phase was removed and the wet cellulose was weighed.

4.3 FT-IR analyses

The IR analyses were performed with a ALPHA compact FT-IR spectrometer (Bruker Optics, Billerica, MA, USA) equipped with the OPUS/Mentor software. Each time, a sample of few mg of lemon or grapefruit CytroCell cellulose in powder form was mixed with ultrapure KBr (FT-IR grade, ≥99% trace metals basis, Sigma-Aldrich, St. Louis, MI, USA). A small amount (ca. 20 mg) of CytroCell was mixed with an excess of KBr powder (ca. 150 mg) and ground using a pestle in an agate mortar to form a uniform mixture. A Specac Mini-Pellet laboratory hydraulic press was used for the preparation of high-quality 7 mm KBr pellets for transmission FTIR (Figure 6) applying a 12 t weight for 5 min.

Figure 6. Pellets of lemon (yellow) and grapefruit (orange) CytroCell dispersed in KBr.

4.4 XRD analysis

The samples were analyzed by a D5005 X-ray diffractometer (Bruker AXS, Karlsruhe, Germany) operating at 40 kV and 30 mA to obtain the diffraction profile at 0.15°/ min acquisition rate over a 5.0°–40.0° 2θ range. The X-ray radiation was generated via a copper (Kα) anode, and made monochromatic via the instrument's secondary monochromator.

4.5 Nitrogen physisorption measurements

The nitrogen adsorption isotherms were obtained using a ASAP 2020 Plus surface area and porosimetry system (Micromeritics Instrument Corporation, Norcross, GA, USA) equipped with the ASAP 2020 Plus Version 1.03 software. An aggregate sample of CytroCell (110.5 mg for grapefruit CytroCell and 93.5 mg for lemon CytroCell) inserted in a glass burette was first degassed by heating it for 10 min with a heating ramp rate of 10°C/min. The analysis was carried out at 77.423 K with a 10 s equilibration interval.

4.6 Disc Preparation

The same hydrated sample obtained after prolonged contact of 200 mg grapefruit or lemon CytroCell cellulose with water after centrifugation in the WRC test, was added with 5 mL distillate water. After short homogenization using a vortex mixer (IKA Vortex 1), the mixture was dried in an oven at 35°C for 20 h.

4.7 Zeta potential

The zeta potential was determined at 25 °C with a Zetasizer Nano ZS analyzer (Malvern Panalytical, Malvern, Great Britain) using a laser wavelength of 633 nm to measure the speed of particle movement, using laser Doppler electrophoresis. A suspension of CytroCell (20 mg) in 10 mL millQ water was employed in the measurements carried out in a DTS1070 cell. The zeta potential reported is the average of three measurements, which returned very similar results.

Acknowledgments: This study is dedicated to the memory of Professor Herman van Bekkum (1932-2020), Technische Universiteit Delft, a pioneer in catalysis research applied to carbohydrate selective conversions. We thank Dr. Nunzio Gabriele Gallì, Istituto per lo Studio dei Materiali Nanostrutturati, CNR, for the nitrogen physisorption measurements. Thanks to OPAC Campisi (Siracusa, Italy) for kindly providing the lemon and grapefruit bagasse from which the CytroCell celluloses were obtained.

Funding: This research received no external funding.

Conflicts of Interest: The authors declare no conflict of interest.

Sample Availability: Samples of the compounds are available from the authors.

ORCID

Antonino Scurria: 0000-0001-5624-6833

Lorenzo Albanese: 0000-0002-4549-8514

Mario Pagliaro: 0000-0002-5096-329X

Federica Zabini: 0000-0003-1505-0839

Francesco Giordano: 0000-0003-3646-3210

Francesco Meneguzzo: 0000-0002-5952-9166

Rosaria Ciriminna: 0000-0001-6596-1572

References

1. J. Á. Siles López, Q. Li, I. P. Thompson, Biorefinery of waste orange peel, *Crit. Rev. Biotechnol.* **2010**, *30*, 63-69. https://doi.org/10.3109/07388550903425201
2. D. A. Zema, P. S. Calabrò, A. Folino, V. Tamburino, G. Zappia, S. M. Zimbone, Valorisation of citrus processing waste: A review, *Waste Manage.* **2018**, *80*, 252–273. https://doi.org/10.1016/j.wasman.2018.09.024
3. I. Bicu, F. Mustata, Optimization of isolation of cellulose from orange peel using sodium hydroxide and chelating agents, *Carbohydr. Polym.* **2013**, *98*, 341-348. https://doi.org/10.1016/j.carbpol.2013.06.009
4. A. M. Santonocito, E. Vismara, Production of textile from citrus fruit, WO2015018711A1.
5. R. C. Rivas-Cantu, K. D. Jones, P. L. Mills, A citrus waste-based biorefinery as a source of renewable energy: technical advances and analysis of engineering challenges, *Waste Manag. Res.* **2013**, *31*, 413–420. https://doi.org/10.1177/0734242x13479432
6. P. Phanthong, P. Reubroycharoen, X. Hao, G. Xu, A. Abudula, G. Guan, Nanocellulose: Extraction and application, *Carbon Resour. Convers.* **2018**, *1*, 32-43. https://doi.org/10.1016/j.crcon.2018.05.004
7. M. Mariño, L. Lopes da Silva, N. Durán, L. Tasic, Enhanced Materials from Nature: Nanocellulose from Citrus Waste, *Molecules* **2015**, *20*, 5908-5923. https://doi.org/10.3390/molecules20045908
8. E. M. de Melo, J. H. Clark, A. S. Matharu, The Hy-MASS concept: hydrothermal microwave assisted selective scissoring of cellulose for *in situ* production of (meso)porous nanocellulose fibrils and crystals, *Green Chem.* **2017**, *19*, 3408-3417. https://doi.org/10.1039/c7gc01378g
9. S. Naz, N. Ahmad, J. Akhtar, N. M. Ahmad, A. Ali, M. Zia, Management of Citrus Waste by switching in the production of nanocellulose, *IET Nanobiotechnol.* **2016**, *10*, 395. http://dx.doi.org/10.1049/iet-nbt.2015.0116
10. A. E. J. de Nooy, A. C. Besemer, H. van Bekkum, On the use of stable organic nitroxyl radicals for the oxidation of primary and secondary alcohols, *Synthesis* **1996**, *10*, 1153-1176. https://doi.org/10.1055/s-1996-4369

11. Stora Enso, MFC for packaging, **2020**. https://www.storaenso.com/en/products/bio-based-materials/mfc-for-packaging (last time accessed, January 7, 2020).
12. S. Jongaroontaprangsee, N. Chiewchan, S. Devahastin, Production of nanocellulose from lime residues using chemical-free technology, *Mater. Today-Proc.* **2018**, *5*, 11095-11100. https://doi.org/10.1016/j.matpr.2018.01.027
13. D. Panda, S. Manickam, Cavitation Technology—The Future of Greener Extraction Method: A Review on the Extraction of Natural Products and Process Intensification Mechanism and Perspectives, *Appl. Sci.* **2019**, *9*, 766. https://doi.org/10.3390/app9040766
14. F. Meneguzzo, C. Brunetti, A. Fidalgo, R. Ciriminna, R. Delisi, L. Albanese, F. Zabini, A. Gori, L. B.dos Santos Nascimento, A. De Carlo, F. Ferrini, L. M. Ilharco, M. Pagliaro, Real-Scale Integral Valorization of Waste Orange Peel via Hydrodynamic Cavitation, *Processes* **2019**, *7*, 581. https://doi.org/10.3390/pr7090581
15. F. Meneguzzo, R. Ciriminna, F. Zabini, M. Pagliaro, Review of Evidence Available on Hesperidin-Rich Products as Potential Tools against COVID-19 and Hydrodynamic Cavitation-Based Extraction as a Method of Increasing Their Production, *Processes* **2020**, *8*, 549. https://doi.org/10.3390/PR8050549
16. D. Nuzzo, L. Cristaldi, M. Sciortino, L. Albanese, A. Scurria, F. Zabini, C. Lino, M. Pagliaro, F. Meneguzzo, M. Di Carlo, R. Ciriminna, Exceptional antioxidant, non-cytotoxic activity of integral lemon pectin from hydrodynamic cavitation, *ChemistrySelect* **2020**, *5*, 5066-5071. https://doi.org/10.1002/slct.202000375
17. A. Presentato, A. Scurria, L. Albanese, C. Lino, M. Sciortino, M. Pagliaro, F. Zabini, F. Meneguzzo, R. Alduina, D. Nuzzo, R. Ciriminna, Superior antibacterial activity of integral lemon pectin from hydrodynamic cavitation, *ChemistryOpen* **2020**, *9*, 628-630. https://doi.org/10.1002/open.202000076
18. A. Presentato, E. Piacenza, A. Scurria, L. Albanese, F. Zabini, F. Meneguzzo, D. Nuzzo, M. Pagliaro, D. Chillura Martino, R. Alduina, R. Ciriminna, A New Water-Soluble Bactericidal Agent for the Treatment of Infections Caused by Gram-Positive and Gram-Negative Bacterial Strains, *Antibiotics* **2020**, *9*, 586. https://doi.org/10.3390/antibiotics9090586
19. M. Thommes, K. Kaneko, A. V. Neimark, J. P. Olivier, F. Rodriguez-Reinoso, J. Rouquerol, K. S.W. Sing, Physisorption of gases, with special reference to the evaluation of surface area and pore size distribution (IUPAC Technical Report), *Pure Appl. Chem.* **2015**, *87*, 1051-1069. https://doi.org/10.1515/pac-2014-1117
20. S.-S. Chang, B. Clair, J. Ruelle, J. Beauchêne, F. Di Renzo, F. Quignard, G.-J. Zhao, H. Yamamoto, J. Gril, Mesoporosity as a new parameter for understanding tension stress generation in trees, *J. Exp. Bot.* **2009**, *60*, 3023-3030. https://doi.org/10.1093/jxb/erp133
21. J. C. Groen, J. Pérez-Ramirez, Critical appraisal of mesopore determination by adsorption analysis, *Appl. Catal. A* **2004**, *268*, 121-125. https://doi.org/10.1016/j.apcata.2004.03.031
22. R.G. Zhbankov, S.P. Firsov, E.V. Korolik, P.T. Petrov, M.P. Lapkovski, V.M. Tsarenkov, M.K. Marchewka, H. Ratajcak, Vibrational spectra and the structure of medical biopolymers, *J. Mol. Struct.* **2000**, *555*, 85-96
23. S. Cichosz, A. Masek, IR Study on Cellulose with the Varied Moisture Contents: Insight into the Supramolecular Structure, *Materials* **2020**, *13*, 4573. https://doi.org/10.3390/ma13204573
24. K. V. Berezin, I. T. Shagautdinova, M. L. Chernavina, A. V. Novoselova, K. N. Dvoretskii, A. M. Likhter, The Experimental Vibrational Infrared Spectrum of Lemon Peel and Simulation of Spectral Propertiesof the Plant Cell Wall, *Opt. Spectrosc.* **2017**, *123*, 495-500. https://doi.org/10.1134/s0030400x17090089
25. S. Y. Oh, D. I. Yoo, Y. Shin, G. Seo, FTIR analysis of cellulose treated with sodium hydroxide and carbon dioxide, *Carbohydr. Res.* **2005**, *340*, 417-428. https://doi.org/10.1016/j.carres.2004.11.027
26. P. Widsten, N. Dooley, R. Parr, J. Capricho, I. Suckling, Citric acid crosslinking of paper products for improved high-humidity performance, *Carbohydr. Polym.* **2014**, *101*, 998-1004. https://doi.org/10.1016/j.carbpol.2013.10.002
27. H. Arslanoglu, H. Soner Altundogan, F. Tumen, Preparation of cation exchanger from lemon and sorption of divalent heavy metals, *Biores. Technol.* **2008**, *99*, 2699-2705. https://doi.org/10.1016/j.biortech.2007.05.022
28. T. J. Bondancia, J. de Aguiar, G. Batista, A. J. G. Cruz, J. M. Marconcini, L. H. C. Mattoso, C. S. Farinas, Production of Nanocellulose Using Citric Acid in a Biorefinery Concept: Effect of the Hydrolysis Reaction Time and Techno-Economic Analysis, *Ind. Eng. Chem. Res.* **2020**, *59*, 11505-11516. https://doi.org/10.1021/acs.iecr.0c01359
29. L. Segal, J. Creely, A. Martin, C. Conrad, An empirical method for estimating the degree of crystallinity of native cellulose using the X-ray diffractometer, *Text. Res. J.* **1962**, *29*, 786-794. https://dx.doi.org/10.1177/004051755902901003

30. A. Scurria, M. Sciortino, A. Presentato, C. Lino, E. Piacenza, L. Albanese, F. Zabini, F. Meneguzzo, D. Nuzzo, M. Pagliaro, D. F. Chillura Martino, R. Alduina, G. Avellone, R. Ciriminna, Volatile Compounds of Lemon and Grapefruit IntegroPectin, *Molecules* **2021**, *26*, 51. https://doi.org/10.3390/molecules26010051
31. P. Satyamurthy, R.H. Balasubramanya, N. Vigneshwaran, Preparation and characterization of cellulose nanowhiskers from cotton fibres by controlled microbial hydrolysis, *Carbohydr. Polym.* **2011**, *83*, 122-129. https://dx.doi.org/10.1016/j.carbpol.2010.07.029
32. G. Karabourniotis, H. T. Horner, P. Bresta, D. Nikolopoulos, G. Liakopoulos, New insights into the functions of carbon-calcium inclusions in plants, *New Phytologist* **2020**, *228*, 845-854. https://doi.org/10.1111/nph.16763
33. S. Bhattacharjee, DLS and zeta potential – What they are and what they are not?, *J. Control. Rel.* **2016**, *235*, 337-351. https://doi.org/10.1016/j.jconrel.2016.06.017
34. J. F. Ang, Water Retention Capacity and Viscosity Effect of Powdered Cellulose, *J. Food Sci.* **1991**, *56*, 1682-1684. https://doi.org/10.1111/j.1365-2621.1991.tb08670.x
35. N. Mahato, K. Sharma, M. Sinha, E. R. Baral, R. Koteswararao, A. Dhyani, M. H. Cho, S. Cho, Bio-sorbents, industrially important chemicals and novel materials from citrus processing waste as a sustainable and renewable bioresource: A review, *J. Adv. Res.* **2020**, *23*, 61-82. https://doi.org/10.1016/j.jare.2020.01.007